



**HAL**  
open science

## **A methyl transferase links the circadian clock to the regulation of alternative splicing**

Sabrina E. Sanchez, Ezequiel Petrillo, Esteban J. Beckwith, Xu Zhang, Mathias L. Rugnone, C. Esteban Hernando, Juan C. Cuevas, Micaela A. Godoy Herz, Ana Depetris-Chauvin, Craig G. Simpson, et al.

► **To cite this version:**

Sabrina E. Sanchez, Ezequiel Petrillo, Esteban J. Beckwith, Xu Zhang, Mathias L. Rugnone, et al.. A methyl transferase links the circadian clock to the regulation of alternative splicing. *Nature*, 2010, 468 (7320), pp.112-116. 10.1038/nature09470 . hal-01218274

**HAL Id: hal-01218274**

**<https://hal.science/hal-01218274>**

Submitted on 20 Oct 2015

**HAL** is a multi-disciplinary open access archive for the deposit and dissemination of scientific research documents, whether they are published or not. The documents may come from teaching and research institutions in France or abroad, or from public or private research centers.

L'archive ouverte pluridisciplinaire **HAL**, est destinée au dépôt et à la diffusion de documents scientifiques de niveau recherche, publiés ou non, émanant des établissements d'enseignement et de recherche français ou étrangers, des laboratoires publics ou privés.

# A methyl transferase links the circadian clock to the regulation of alternative splicing

Sabrina E. Sanchez<sup>1\*</sup>, Ezequiel Petrillo<sup>2\*</sup>, Esteban J. Beckwith<sup>3</sup>, Xu Zhang<sup>4</sup>, Matias L. Rugnone<sup>1</sup>, C. Esteban Hernando<sup>1</sup>, Juan C. Cuevas<sup>5</sup>, Micaela A. Godoy Herz<sup>2</sup>, Ana Depetris-Chauvin<sup>3</sup>, Craig G. Simpson<sup>6</sup>, John W. S. Brown<sup>6,7</sup>, Pablo D. Cerdán<sup>3</sup>, Justin O. Borevitz<sup>4</sup>, Paloma Mas<sup>5</sup>, M. Fernanda Ceriani<sup>3</sup>, Alberto R. Kornblihtt<sup>2</sup> & Marcelo J. Yanovsky<sup>1,3</sup>

Circadian rhythms allow organisms to time biological processes to the most appropriate phases of the day–night cycle<sup>1</sup>. Post-transcriptional regulation is emerging as an important component of circadian networks<sup>2–6</sup>, but the molecular mechanisms linking the circadian clock to the control of RNA processing are largely unknown. Here we show that PROTEIN ARGININE METHYL TRANSFERASE 5 (PRMT5), which transfers methyl groups to arginine residues present in histones<sup>7</sup> and Sm spliceosomal proteins<sup>8,9</sup>, links the circadian clock to the control of alternative splicing in plants. Mutations in *PRMT5* impair several circadian rhythms in *Arabidopsis thaliana* and this phenotype is caused, at least in part, by a strong alteration in alternative splicing of the core-clock gene *PSEUDO RESPONSE REGULATOR 9* (*PRR9*). Furthermore, genome-wide studies show that PRMT5 contributes to the regulation of many pre-messenger-RNA splicing events, probably by modulating 5′-splice-site recognition. *PRMT5* expression shows daily and circadian oscillations, and this contributes to the mediation of the circadian regulation of expression and alternative splicing of a subset of genes. Circadian rhythms in locomotor activity are also disrupted in *dart5-1*, a mutant affected in the *Drosophila melanogaster* *PRMT5* homologue, and this is associated with alterations in splicing of the core-clock gene *period* and several clock-associated genes. Our results demonstrate a key role for PRMT5 in the regulation of alternative splicing and indicate that the interplay between the circadian clock and the regulation of alternative splicing by PRMT5 constitutes a common mechanism that helps organisms to synchronize physiological processes with daily changes in environmental conditions.

The circadian clock interacts with light to inhibit stem elongation in plants<sup>10</sup>, so we used tall plants under conditions of a light–dark cycle to identify novel clock mutants. This screening, combined with a positional cloning approach, allowed us to find a mutation in *PRMT5* that lengthened the period of circadian rhythms in leaf movement and gene expression in *Arabidopsis* (Fig. 1a, b and Supplementary Fig. 1). The same phenotype was observed in other loss-of-function alleles of *PRMT5* (Supplementary Fig. 1).

The core oscillator in *Arabidopsis* depends on the interaction between the Myb transcription factors CIRCADIAN CLOCK ASSOCIATED 1 (*CCA1*) and LATE ELONGATED HYPOCOTYL (*LHY*), and the PSEUDO-RESPONSE REGULATOR 1 (*PRR1*) (also known as TIMING OF CAB EXPRESSION 1 (*TOC1*))<sup>11</sup>. We observed that *prmt5* mutants had a longer circadian period of *TOC1* expression than wild-type plants (Fig. 1c and Supplementary Fig. 2), and a delayed expression of *TOC1* in a light–dark cycle (Supplementary Fig. 2). We observed similar alterations in *LHY* and *CCA1* expression (Supplementary Fig. 3). Interestingly, *PRMT5* expression was regulated by the circadian clock (Fig. 1d and Supplementary Fig. 4), indicating that it is part of a feedback loop controlling clock function in *Arabidopsis*.

PRMT5 methylates histone 4 in *Arabidopsis* and regulates flowering time through the epigenetic repression of *FLOWERING LOCUS C* (*FLC*)<sup>12–14</sup>. *FLC* regulates circadian rhythms at high temperatures<sup>15</sup>, but genetic analysis indicated that *prmt5* affects circadian rhythms independently of *FLC* (Supplementary Fig. 5). Next we explored the connection between PRMT5 and the circadian network more thoroughly using Affymetrix expression arrays. Clock-regulated genes<sup>15</sup> were over-represented among PRMT5 targets at the mRNA level (1.7-fold enrichment;  $P < 3 \times 10^{-11}$ ). Indeed, genes upregulated in *prmt5* mutants were enriched in those with peak expression during daytime, and genes downregulated were enriched in those with peak expression during night time (Supplementary Fig. 6). More interestingly, the gene showing the largest enhancement in expression was *PRR9* (Supplementary Fig. 7a and Supplementary Table 1), a homologue of *TOC1/PRR1* that acts redundantly with *PRR7* to repress *CCA1* and *LHY* expression<sup>16</sup>. *PRR7* mRNA levels were also increased in *prmt5-5* mutants (Supplementary Table 2). Quantitative polymerase chain reaction (qPCR) analysis confirmed increased *PRR9* mRNA levels in *prmt5-5* plants, particularly in the late subjective day (Supplementary Fig. 7b). Overexpression of *PRR9*, however, shortens rather

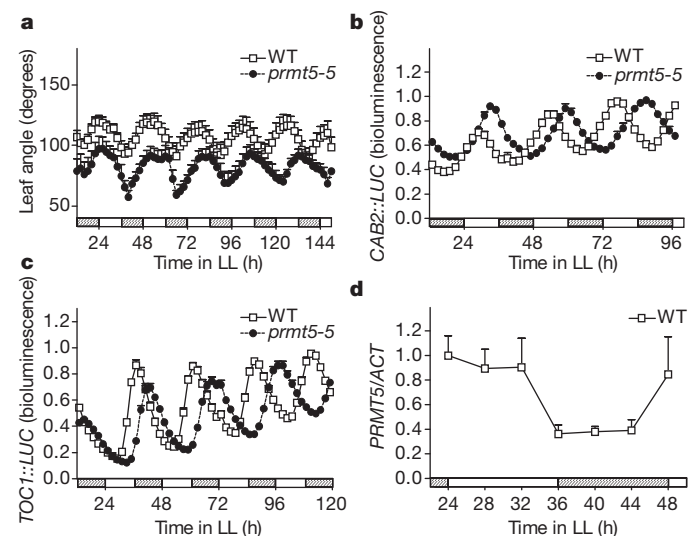


**Figure 1 | A role for PRMT5 in the circadian system of *Arabidopsis*.** **a**, Circadian rhythm of leaf movement in constant light (LL) (h, hours;  $n = 6$ ). WT, wild type. **b**, **c**, Bioluminescence analysis of *CAB2::LUC* expression ( $n = 7–10$ ) (**b**) or *TOC1::LUC* expression ( $n = 8–10$ ) (**c**). **d**, *PRMT5* expression measured by qPCR in constant light ( $n = 4$ ) relative to *ACTIN 8* (*ACT*). Data represent average  $\pm$  s.e.m. Open squares, wild type; filled circles, *prmt5* mutant. Open and lined boxes indicate subjective day or night, respectively.

<sup>1</sup>IFEVA, Facultad de Agronomía, UBA-CONICET, C1417DSE Buenos Aires, Argentina. <sup>2</sup>FIBYNE, FCEyN, UBA-CONICET, C1428EGA Buenos Aires, Argentina. <sup>3</sup>Fundación Instituto Leloir, IIBBA-CONICET, C1405BWE Buenos Aires, Argentina. <sup>4</sup>Department of Ecology & Evolution, University of Chicago, Chicago, Illinois 60637, USA. <sup>5</sup>Centre for Research in Agricultural Genomics (CRAG), Consortium CSIC-IRTA-UAB, Barcelona 08034, Spain. <sup>6</sup>Genetics Programme, SCRI, Invergowrie, Dundee DD2 5DA, UK. <sup>7</sup>Division of Plant Sciences, University of Dundee at SCRI, Dundee, DD2 5DA, UK.

\*These authors contributed equally to this work.

than lengthens the period of circadian rhythms<sup>17</sup>. Furthermore, we could not detect a PRMT5 epigenetic mark<sup>7</sup> in *PRR9* (Supplementary Fig. 8), indicating that circadian alterations in *prmt5* do not result from defective epigenetic repression of *PRR9*.

In addition to histones, PRMT5 (also known as DART5/CSUL) symmetrically dimethylates Sm proteins in *Drosophila*<sup>8,9</sup> and we obtained similar evidence in *Arabidopsis* (Supplementary Fig. 9). Indeed, PRMT5 acts together with the survival motor neuron (SMN) complex to regulate spliceosome assembly in human cells<sup>18</sup>, and mutations in *SMN* have been shown to affect alternative splicing in a tissue-specific manner in mice<sup>19</sup>. However, the lack of symmetrical dimethylation of Sm proteins in *prmt5* mutant flies does not impair small nuclear ribonucleoprotein particle (snRNP) assembly<sup>20</sup>. Therefore, if and how PRMT5 contributes to the regulation of pre-mRNA splicing is uncertain.

Besides complementary DNAs encoding the full-length *PRR9* protein, splice variants that retain intron 3 and/or use an alternative 5' splice site at the end of exon 2 have been reported (Fig. 2a). A PCR preceded by a reverse transcription reaction (RT-PCR) conducted to evaluate the relative abundance of all *PRR9* mRNA isoforms revealed significant alterations in alternative splicing in *prmt5* mutants (Fig. 2a and Supplementary Fig. 10). qPCR confirmed that *prmt5* seedlings had increased levels of an isoform that retains intron 3 (Fig. 2b), but greatly reduced levels of the isoform encoding the full-length protein (Fig. 2c). No effect on circadian rhythmicity was observed in plants overexpressing *PRR9\_B* mRNA, which encodes a truncated protein identical to that of *PRR9\_D* mRNA (Supplementary Fig. 11). On the other hand, reduced levels of the

functional *PRR9* mRNA isoform may contribute to the phenotype of the mutant, as *prmt5-5* delayed the pace of the clock on a wild-type background but did not affect circadian period on a *prr9;prr7* background, where the function of *PRR9* is most evident owing to its redundancy with *PRR7*<sup>16</sup> (Fig. 2d). Interestingly, *PRR9\_A* and *PRR9\_B* mRNAs, the most abundant isoforms in wild-type plants, oscillate with slightly different phases (Supplementary Fig. 12), indicating that this may contribute to refining the shape of *PRR9* oscillation, ensuring that repression of *CCA1* and *LHY* expression begins after dawn. Changes in alternative splicing of *PRR9*, however, are unlikely to account for all the effect of *prmt5* on circadian rhythms, as both *PRR9* and *PRR7* are required for PRMT5 effects on the clock (Fig. 2d) and PRMT5 affects *PRR7* expression (Supplementary Table 2 and Supplementary Fig. 13) but not its splicing (data not shown). Taken together, these results indicate that PRMT5 affects circadian rhythms in *Arabidopsis*, regulating *PRR9* alternative splicing as well as the timing of expression and/or function of *PRR7*.

Next we analysed the effects of PRMT5 on pre-mRNA splicing at a genome-wide level using Affymetrix tiling arrays. We identified 471 introns, out of a total of 67,791, with significantly higher hybridization signals in *prmt5* mutants (Supplementary Table 3). The increased signal for these introns probably reflects intron retention, as most of the other introns and exons within these genes did not differ between wild-type and mutant plants (Fig. 3a). These results were confirmed for a subset of genes by conventional RT-PCR (Supplementary Fig. 14). To determine changes in alternative splicing in more detail we used a high-resolution RT-PCR panel that included several known alternative splicing events<sup>21,22</sup>. *prmt5* mutants had significant alterations in 44 out of 288 events analysed (Supplementary Table 4), which included exon skipping, alternative donor and acceptor splice sites, as well as intron retention (Fig. 3b and Supplementary Table 4). Interestingly, *PRR9* was one of the genes showing the largest alterations in alternative splicing in *prmt5* mutants (Supplementary Table 4 and Supplementary Fig. 15). The fact that PRMT5 regulated approximately 15% of the alternative splicing events analysed through the high-resolution RT-PCR panels, but only a minor proportion of introns evaluated using tiling arrays (less than 1%), indicates that this protein has specific functions regulating splice-site selection rather than a role in constitutive pre-mRNA splicing. Interestingly, we found a significant enrichment in alternative 5' splice sites among all splicing events affected in *prmt5* mutants (Fig. 3c). A defect in 5'-splice-site recognition should also cause retention of some introns and, indeed, all the splicing defects detected using tiling arrays corresponded to increased intron retention (Supplementary Table 3). A comparison between the 5' splice site of the splicing events most significantly affected in *prmt5* mutants (Supplementary Table 5) and the *Arabidopsis* 5'-splice-site consensus sequence, revealed an important decrease in the frequency of the dominant G at the -1 position and a tendency towards randomization of the nucleotides present at the -2, -1 and +5 positions (Fig. 3d). Thus, these observations strongly indicate that PRMT5 regulates alternative splicing, contributing, at least in part, to the recognition of weak 5' splice sites.

Given that the circadian clock regulates *PRMT5* expression and that PRMT5 contributes to modulate alternative splicing, we proposed that PRMT5 may link the circadian clock to the regulation of alternative splicing. To evaluate this possibility in detail we analysed alternative splicing of *RUBISCO ACTIVASE (RCA)* under light-dark-cycle and free-running conditions. *RCA* produces a short mRNA encoding a protein whose activity is regulated by light intensity and a long mRNA that arises through the usage of an alternative donor site, encoding a protein that is not regulated by light<sup>23</sup>. Our RT-PCR analysis confirmed the alterations in *RCA* alternative splicing observed in *prmt5-5* using the high-resolution RT-PCR panel (Fig. 3e). Furthermore, we found that the ratio between the mRNA levels of the two *RCA* splice variants showed daily and circadian oscillations in wild-type *Arabidopsis*. These oscillations seem to be physiologically relevant, as the relative proportion of the short mRNA, encoding the protein whose activity is regulated by light intensity, increased during daytime (Fig. 3f).

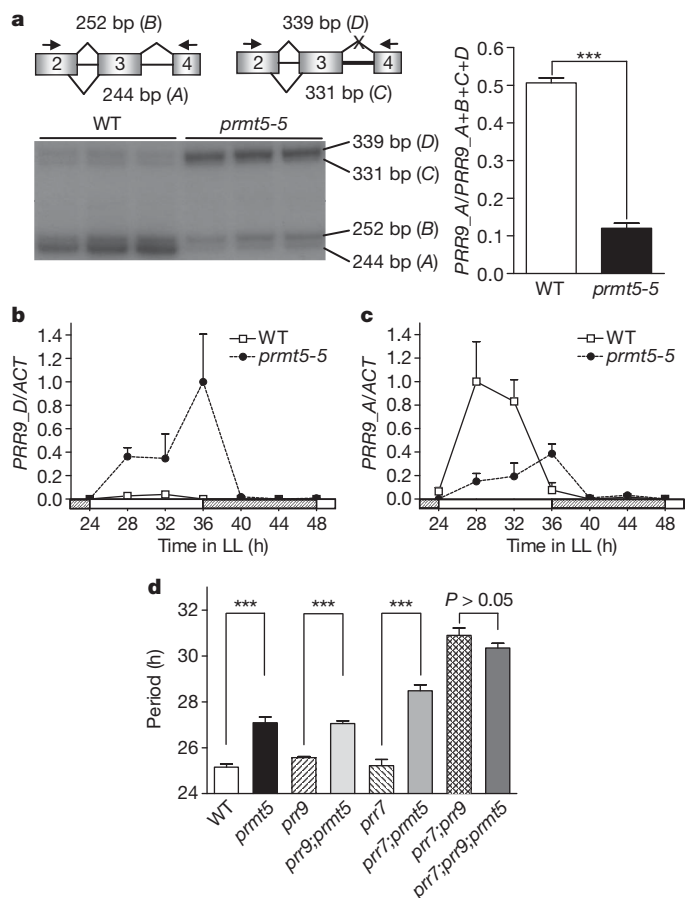


**Figure 2** | PRMT5 affects expression and alternative splicing of the clock gene *PRR9*. **a**, *PRR9* splice variants (*PRR9\_A* to *PRR9\_D*) and their relative abundance measured by radioactive PCR (\*\*\*)  $P < 0.0001$ ;  $n = 3$ ). bp, base pairs. **b**, **c**, Expression of *PRR9\_D* (**b**) and *PRR9\_A* (**c**) by qPCR in constant light ( $n = 4$ ). **d**, Free-running period of leaf movement (\*\*\*)  $P < 0.001$ ;  $n = 6$ ). Data represents average + s.e.m. Open squares, wild type; filled circles, *prmt5* mutant.

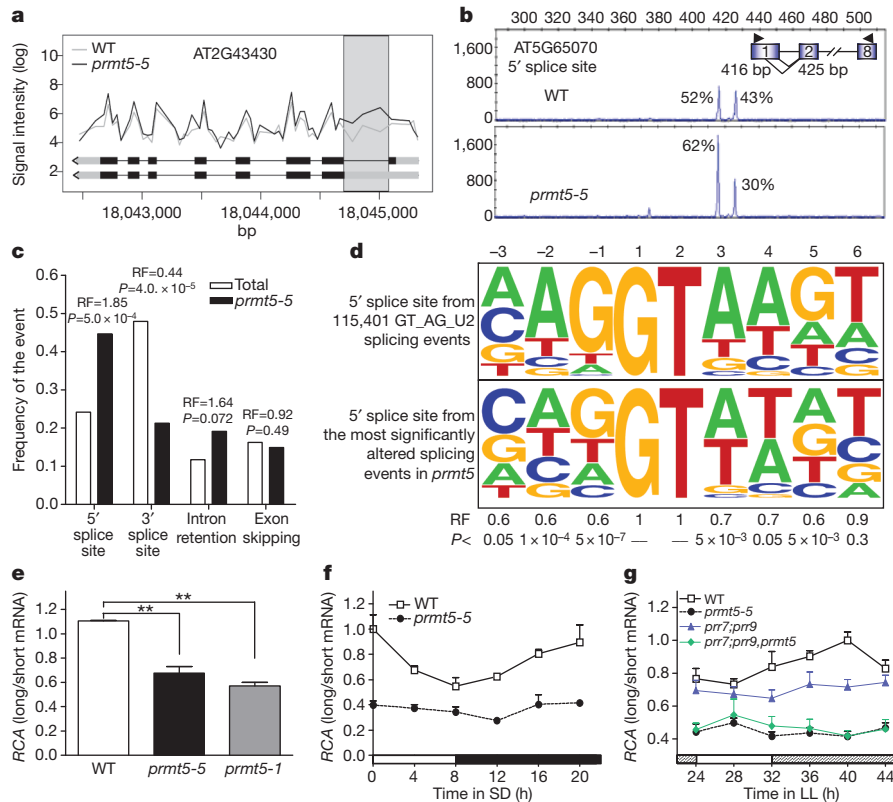


**Figure 3 | Genome-wide analysis of pre-mRNA splicing in *Arabidopsis prmt5* mutants.** **a**, Tiling array data of a representative gene with an alteration in pre-mRNA splicing in *prmt5* mutants ( $n = 3$ ). **b**, Example of a high-resolution RT-PCR reaction shown as an electropherogram depicting splicing pattern changes in *prmt5-5*. Percentage of each isoform relative to the total is shown. **c**, Frequency of each type of alternative splicing event in the high-resolution RT-PCR panel (total) and among those altered in *prmt5-5*. The representation factor (RF) is the frequency in *prmt5-5* divided by the total frequency. **d**, Pictograms showing the frequency distribution of nucleotides at

the 5' splice site of 115,401 *Arabidopsis* introns (top), and in the 50 splicing events most significantly altered in *prmt5-5* (bottom). **e–g**, RCA splice variants in plants grown always in constant light (\*\* $P < 0.01$ ) (**e**), in a short-day cycle (SD; 8:16 h light–dark) (**f**) or in seedlings transferred to constant light after entrainment in a light–dark cycle (**g**). Values are average + s.e.m. ( $n = 3–4$ ). Open squares, wild type; filled circles, *prmt5-5*; uptriangles, *prp7;prp9*; diamonds, *prp7;prp9;prmt5*. Open and closed boxes indicate light and dark period, respectively. Lined boxes indicate subjective night.

Circadian oscillations in RCA alternative splicing were disrupted in *prmt5* seedlings and, more importantly, alterations in the ratio of the two mRNA isoforms were more severe in *prmt5* and *prmt5;prp9;prp7* than in *prp9;prp7* mutants, indicating a direct role for PRMT5 in the control of this process rather than an indirect role through its effect on circadian rhythms (Fig. 3g). Circadian oscillations in alternative splicing were also observed for *RSP31*, but not for *AT5G57630*, two alternatively spliced genes regulated by PRMT5 according to high-resolution RT-PCR analysis (Supplementary Fig. 16). Lack of oscillation of some PRMT5 targets may be due to enhanced stability of the corresponding mRNAs.

Two mutant alleles affected in the *D. melanogaster prmt5* gene, *dart5-1* and *csul<sup>RM50</sup>*, have been identified<sup>8,9</sup>, and allowed us to evaluate the effects of PRMT5 on the circadian system and splicing regulation in this organism. Compared to heterozygous controls, homozygous *dart5* mutants showed poor rhythms in locomotor activity in a light–dark cycle and decreased rhythmicity in constant darkness (Fig. 4a, b). Similar alterations were observed for *csul<sup>RM50</sup>* (Supplementary Fig. 17). However, we observed strong oscillations in the expression of core-clock genes and in PERIOD (PER) protein levels (Fig. 4c, d and Supplementary Fig. 18), indicating that PRMT5 modulates behavioural rhythms and thus controls the mechanism linking the central oscillator to clock output, rather than through effects on the core oscillator.

Next we evaluated pre-mRNA splicing of clock and non-clock genes in *Drosophila*. Circadian regulation of alternative splicing of the core-clock gene *per* has been reported to have an important role in adjusting circadian rhythms to changes in photoperiod and temperature in *Drosophila*<sup>5,6</sup>. Interestingly, we observed circadian oscillations in the

ratio of the two *per* mRNA variants<sup>5</sup> in wild-type flies (that is, intron-8-retained A or a spliced variant B'), whereas mostly B' was present in *dart5-1* flies independently of the time of day (Fig. 4e). We also conducted a genome-wide analysis of pre-mRNA splicing using tiling arrays and found 418 introns whose hybridization signal increased in *dart5-1*, several of which were confirmed by qPCR (Fig. 4f), and 30 introns that showed higher signals in wild-type flies (Supplementary Table 6). Among the genes that showed increased intron retention in *dart5-1* we found *takeout* (*to*) and *slowpoke*, two genes implicated in the regulation of clock outputs in *Drosophila*<sup>24,25</sup>, as well as *norpA*, a phospholipase C that regulates clock entrainment<sup>26</sup> and *per* splicing (Supplementary Table 6)<sup>5,6,26</sup>. There were also differences in the expression of 65 exons corresponding to genes whose remaining exons, in most cases, did not show differences in their overall levels (Supplementary Table 7). In contrast to *dart5-1*, the arrhythmic mutants *per<sup>01</sup>* and *clk<sup>irk</sup>* did not show large alterations in splicing, at least for the events evaluated here, indicating that changes in splicing in *dart5-1* are not simply the indirect consequence of arrhythmicity (Supplementary Fig. 19).

Similar to the findings in *Arabidopsis*, we observed a reduction in the frequency of the dominant G –1 nucleotide in the 5'-splice-site sequences of the most significantly affected splicing events in *dart5-1* (Fig. 4g and Supplementary Table 8). Taken together, these results strongly indicate that PRMT5 regulates pre-mRNA splicing, affecting the efficiency with which snRNPs interact with certain splice sites. Recognition of 5' splice sites involves direct RNA–RNA interactions between the 5' end of the U1 small nuclear RNA and the 5'-splice-site sequence of the target mRNAs. SmB, Smd1 and Smd3 make direct

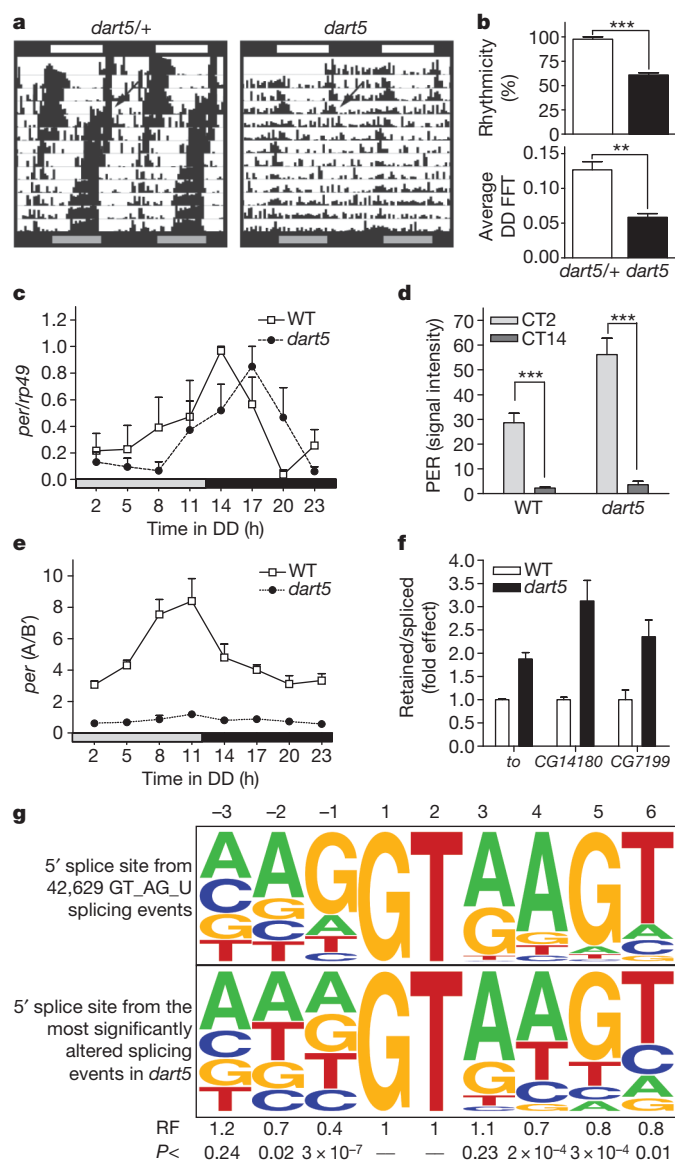


**Figure 4** | PRMT5 regulates circadian rhythms and pre-mRNA splicing in *Drosophila*. **a**, Representative double-plotted actograms. Arrows indicate transfer to constant darkness (DD). **b**, Percentage of rhythmic flies (top) and power fast Fourier transform (FFT) (bottom). \*\*\* $P < 0.001$ , \*\* $P < 0.01$ ;  $n = 70$ . **c**, *per* expression measured by qPCR in constant darkness ( $n = 4$ ). **d**, Nuclear PER immunoreactivity on the small ventral lateral neurons of the *Drosophila* brain in constant darkness. \*\*\* $P < 0.0001$  ( $n \geq 17$ ). CT, circadian time. **e**, Relative levels of A and B' *per* mRNA isoforms over a circadian cycle in constant darkness ( $n = 4$ ). **f**, Radioactive PCR validation of intron retention events for several genes identified using tiling arrays. **g**, Pictograms showing the frequency distribution of nucleotides at the 5' splice site of 42,629 introns in wild-type *Drosophila* genes (top) and in the 50 splicing events most significantly altered in *dart5* (bottom). RF is the frequency observed in *dart5* affected events divided by the genome-wide frequency. **b–f**, Data are average  $\pm$  s.e.m. Open squares, wild type ( $w^{1118}$ ); filled circles, *dart5* (*dart5-1*). **a**, **c**, **e**, black and white boxes represent night and day phases, respectively. Grey bars, subjective day.

contact with the pre-mRNA substrate, close to the 5' splice site and act by stabilizing RNA–RNA interactions in yeast<sup>27</sup>. Thus, methylation of Sm proteins by PRMT5 in plants and flies may facilitate recognition of a subset of 5' splice sites, stabilizing weak RNA–RNA interactions between the U1 snRNA and the 5' splice site of target mRNA. However, we cannot exclude the possibility that some alterations in alternative splicing result from direct or indirect epigenetic defects in *prmt5* mutants<sup>28</sup>.

We also evaluated global effects of PRMT5 on gene expression in *Drosophila* and found 315 genes downregulated and 85 genes upregulated in *dart5-1* (Supplementary Table 9), including a ninefold increase in the mRNA levels of *to* (Supplementary Fig. 20). In contrast to *Arabidopsis*, we did not observe an over-representation of circadianly regulated genes among PRMT5 target genes in *Drosophila* (Supplementary Fig. 21). This was consistent with the lack of circadian regulation of *prmt5/dart5* expression in *Drosophila* (Supplementary Fig. 22). Nonetheless, we did observe a strong enrichment in genes regulated by the core oscillator component CLOCK among PRMT5-regulated genes<sup>29</sup> (Supplementary Fig. 23 and Supplementary Table 10). Thus, although PRMT5 is less tightly linked to the circadian system in *Drosophila* compared to what we observed for PRMT5 in *Arabidopsis*, it is still deeply associated with the fly circadian network controlling behavioural rhythms, splicing of clock-associated genes, and expression of a subset of output genes regulated by the protein CLOCK.

Despite general similarities in the molecular architecture of circadian networks across distantly related organisms, a lack of homology between most clock components indicates an independent evolutionary origin of circadian systems. The existence of a few genes with common roles modulating circadian rhythms in plants and animals<sup>30</sup> probably reflects convergent evolutionary processes associated with a limited number of proteins capable of adapting complex signalling networks to common environmental challenges. The dual role of PRMT5 as an epigenetic regulator of gene expression and as a regulator of alternative splicing makes this protein an ideal tool to link a diverse set of molecular and physiological processes to a central oscillatory system, helping organisms to adjust their growth and development to daily changes in their environment.

## METHODS SUMMARY

**Plant material and physiological assays.** All the *Arabidopsis* lines used in this study were Columbia ecotype. Seedlings were grown at a constant temperature of 22 °C under different light regimes depending on the experiment. Detailed information about flowering time, leaf movement and bioluminescence assays is found in Methods.

***Drosophila* behavioural assays.** Flies were grown and maintained at 25 °C and kept in 12:12 h light–dark cycles. Activity was monitored in a light–dark cycle for 4 days and then in constant darkness for 8 days. Data were collected using activity monitors (TriKinetics). Rhythmicity and fast Fourier transform (FFT) analysis were performed using the ClockLab software (Actimetrics) from data collected in constant darkness.

**Genome tiling array analysis.** Total RNA was processed and hybridized to GeneChip *Arabidopsis* ATH1 Genome Arrays, GeneChip *Arabidopsis* Tiling 1.0R Array, or GeneChip *Drosophila* Tiling 1.0R Array (Affymetrix) according to the manufacturer's instructions. Detailed information about statistical analysis is found in Methods.

**qRT–PCR expression analysis.** RQ1 RNase-Free DNase (Promega) treated RNA samples were subjected to retrotranscription using Invitrogen SuperScript III and oligo-dT. Synthesized cDNAs were amplified with FastStart Universal SYBR Green Master (Roche) using the 7500 Real Time PCR System (Applied Biosystems) cyclor. *ACTIN 8* and *ribosomal protein 49* (*rp49*) transcripts were used as house-keeping for *Arabidopsis* and *Drosophila*, respectively.

**Full Methods** and any associated references are available in the online version of the paper at [www.nature.com/nature](http://www.nature.com/nature).

Received 18 September 2009; accepted 1 September 2010.

Published online 20 October 2010.

- Young, M. W. & Kay, S. A. Time zones: a comparative genetics of circadian clocks. *Nature Rev. Genet.* **2**, 702–715 (2001).
- Hazen, S. *et al.* Exploring the transcriptional landscape of plant circadian rhythms using genome tiling arrays. *Genome Biol.* **10**, R17 (2009).
- Schoning, J. C., Streitner, C., Meyer, I. M., Gao, Y. & Staiger, D. Reciprocal regulation of glycine-rich RNA-binding proteins via an interlocked feedback loop coupling alternative splicing to nonsense-mediated decay in *Arabidopsis*. *Nucleic Acids Res.* **36**, 6977–6987 (2008).
- Guo, J., Cheng, P., Yuan, H. & Liu, Y. The exosome regulates circadian gene expression in a posttranscriptional negative feedback loop. *Cell* **138**, 1236–1246 (2009).

5. Majercak, J., Chen, W. & Edery, I. Splicing of the *period* gene 3'-terminal intron is regulated by light, circadian clock factors, and phospholipase C. *Mol. Cell. Biol.* **24**, 3359–3372 (2004).
6. Collins, B. H., Rosato, E. & Kyriacou, C. P. Seasonal behavior in *Drosophila melanogaster* requires the photoreceptors, the circadian clock, and phospholipase C. *Proc. Natl Acad. Sci. USA* **101**, 1945–1950 (2004).
7. Bedford, M. & Richard, S. Arginine methylation: an emerging regulator of protein function. *Mol. Cell* **18**, 263–272 (2005).
8. Gonsalvez, G., Rajendra, T., Tian, L. & Matera, A. The Sm-protein methyltransferase, Dart5, is essential for germ-cell specification and maintenance. *Curr. Biol.* **16**, 1077–1089 (2006).
9. Anne, J., Olo, R., Ephrussi, A. & Mechler, B. Arginine methyltransferase Capsuléen is essential for methylation of spliceosomal Sm proteins and germ cell formation in *Drosophila*. *Development* **134**, 137–146 (2007).
10. Nozue, K. *et al.* Rhythmic growth explained by coincidence between internal and external cues. *Nature* **448**, 358–361 (2007).
11. Alabadi, D. *et al.* Reciprocal regulation between TOC1 and LHY/CCA1 within the *Arabidopsis* circadian clock. *Science* **293**, 880–883 (2001).
12. Pei, Y. *et al.* Mutations in the type II protein arginine methyltransferase AtPRMT5 result in pleiotropic developmental defects in *Arabidopsis*. *Plant Physiol.* **144**, 1913–1923 (2007).
13. Schmitz, R., Sung, S. & Amasino, R. Histone arginine methylation is required for vernalization-induced epigenetic silencing of FLC in winter-annual *Arabidopsis thaliana*. *Proc. Natl Acad. Sci. USA* **105**, 411–416 (2008).
14. Wang, X. *et al.* SKB1-mediated symmetric dimethylation of histone H4R3 controls flowering time in *Arabidopsis*. *EMBO J.* **26**, 1934–1941 (2007).
15. Edwards, K. D. *et al.* FLOWERING LOCUS C mediates natural variation in the high-temperature response of the *Arabidopsis* circadian clock. *Plant Cell* **18**, 639–650 (2006).
16. Farré, E. M., Harmer, S. L., Harmon, F. G., Yanovsky, M. J. & Kay, S. A. Overlapping and distinct roles of *PRR7* and *PRR9* in the *Arabidopsis* circadian clock. *Curr. Biol.* **15**, 47–54 (2005).
17. Matsushika, A., Imamura, A., Yamashino, T. & Mizuno, T. Aberrant expression of the light-inducible and circadian-regulated *APRR9* gene belonging to the circadian-associated *APRR1/TOC1* quintet results in the phenotype of early flowering in *Arabidopsis thaliana*. *Plant Cell Physiol.* **43**, 833–843 (2002).
18. Chari, A. *et al.* An assembly chaperone collaborates with the SMN complex to generate spliceosomal SnRNPs. *Cell* **135**, 497–509 (2008).
19. Zhang, Z. *et al.* SMN deficiency causes tissue-specific perturbations in the repertoire of snRNAs and widespread defects in splicing. *Cell* **133**, 585–600 (2008).
20. Gonsalvez, G. B., Praveen, K., Hicks, A. J., Tian, L. & Matera, A. G. Sm protein methylation is dispensable for snRNP assembly in *Drosophila melanogaster*. *RNA* **14**, 878–887 (2008).
21. Simpson, C. G. *et al.* Monitoring changes in alternative precursor messenger RNA splicing in multiple gene transcripts. *Plant J.* **53**, 1035–1048 (2008).
22. Raczynska, K. D. *et al.* Involvement of the nuclear cap-binding protein complex in alternative splicing in *Arabidopsis thaliana*. *Nucleic Acids Res.* **38**, 265–278 (2010).
23. Zhang, N., Kallis, R. P., Ewy, R. G. & Portis, A. R. Light modulation of Rubisco in *Arabidopsis* requires a capacity for redox regulation of the larger Rubisco activase isoform. *Proc. Natl Acad. Sci. USA* **99**, 3330–3334 (2002).
24. Sarov-Blat, L., So, W., Liu, L. & Rosbash, M. The *Drosophila* takeout gene is a novel molecular link between circadian rhythms and feeding behavior. *Cell* **101**, 647–656 (2000).
25. Ceriani, M. F. *et al.* Genome-wide expression analysis in *Drosophila* reveals genes controlling circadian behavior. *J. Neurosci.* **22**, 9305–9319 (2002).
26. Glaser, F. T. & Stanewsky, R. Temperature synchronization of the *Drosophila* circadian clock. *Curr. Biol.* **15**, 1352–1363 (2005).
27. Zhang, D., Abovich, N. & Rosbash, M. A biochemical function for the Sm complex. *Mol. Cell* **7**, 319–329 (2001).
28. Schor, I. E., Rascovan, N., Pelisch, F., Alló, M. & Kornblihtt, A. R. Neuronal cell depolarization induces intragenic chromatin modifications affecting NCAM alternative splicing. *Proc. Natl Acad. Sci. USA* **106**, 4325–4330 (2009).
29. McDonald, M. & Rosbash, M. Microarray analysis and organization of circadian gene expression in *Drosophila*. *Cell* **107**, 567–578 (2001).
30. Rosbash, M. The implications of multiple circadian clock origins. *PLoS Biol.* **7**, e62 (2009).

**Supplementary Information** is linked to the online version of the paper at [www.nature.com/nature](http://www.nature.com/nature).

**Acknowledgements** We thank E. M. Farré and S. L. Harmer for seeds; J. J. Casal and S. Mora-García for critical reading of the manuscript; the laboratories of A.R.K. and M.J.Y. for discussions; J. Fuller and P. Tondi for technical assistance. This work was supported by grants from the Fundación Antorchas, the Agencia Nacional de Promoción de Ciencia y Tecnología of Argentina, the Consejo Nacional de Investigaciones Científicas y Técnicas of Argentina and the University of Buenos Aires to M.J.Y. and A.R.K., and from the European Union Network of Excellence on Alternative Splicing (EURASNET) to A.R.K. and J.W.S.B. M.J.Y. and A.R.K. are Howard Hughes Medical Institute international research scholars. P.M.'s laboratory is supported by a Ministerio de Educación y Ciencia grant, the European Young Investigator Awards and the EMBO Young Investigator Awards; M.F.C.'s laboratory is supported by Proyecto de Investigación Científica y Tecnológica 2006-1249.

**Author Contributions** S.E.S. and E.P. contributed equally to this work and performed most of the experiments in this study, with technical assistance from M.L.R., C.E.H., M.A.G.H. and P.D.C. J.C.C. and P.M. conducted bioluminescence and chromatin immunoprecipitation assays. E.J.B. and A.D.C. performed locomotor activity assays, RNA extractions and immunostaining experiments in *Drosophila*. E.P., C.G.S. and J.W.S.B. performed high-resolution RT-PCR experiments. X.Z. and J.O.B. analysed tiling array data. S.E.S., E.P., M.F.C., A.R.K. and M.J.Y. provided input in the preparation of the manuscript, and S.E.S., E.P. and M.J.Y. wrote the paper.

**Author Information** The data discussed in this publication have been deposited in the National Center for Biotechnology Information Gene Expression Omnibus and are accessible through GEO Series accession number GSE18808 (<http://www.ncbi.nlm.nih.gov/geo/query/acc.cgi?acc=GSE18808>). Reprints and permissions information is available at [www.nature.com/reprints](http://www.nature.com/reprints). The authors declare no competing financial interests. Readers are welcome to comment on the online version of this article at [www.nature.com/nature](http://www.nature.com/nature). Correspondence and requests for materials should be addressed to M.J.Y. ([yanovsky@agro.uba.ar](mailto:yanovsky@agro.uba.ar)).

## METHODS

**Plant material and growth conditions.** All the *Arabidopsis* lines used in this study were Columbia ecotype. Seedlings were grown at a constant temperature of 22 °C under different light regimes depending on the experiment. The *prmt5-5* mutant was isolated from a pool of transfer DNA (T-DNA) mutagenized plants (stock no. CS31100 from the Arabidopsis Biological Research Center (ABRC)). The mutation causing the circadian phenotype was not linked to a T-DNA and was identified by positional cloning and sequencing. The *flc* (SALK\_092716), *atprmt5-1* (SALK\_065814) and *atprmt5-2* (SALK\_095085) mutants were obtained from ABRC<sup>31</sup>. Seeds were stratified for four days in the dark at 4 °C and then sown onto either soil or solid Murashige and Skoog medium<sup>32</sup> containing 1% agarose. ***Drosophila* strains and behavioural assays.** Flies were grown and maintained at 25 °C and kept in a 12:12 h light–dark cycle. Activity was monitored in a light–dark cycle for 4 days. Then, flies were released into constant darkness for 8 days. Data were collected using commercially available *Drosophila* activity monitors (TriKinetics). Rhythmicity and FFT analysis were performed using the ClockLab software (Actimetrics) from data collected in constant darkness. *w<sup>1118</sup>* flies used as wild-type controls were provided by the Bloomington Stock Center. The *dart5-1 Drosophila* line was provided by G. Matera and the *csul<sup>RM50</sup>* *Drosophila* line was provided by J. Anne. *per<sup>01</sup>* and *clk<sup>rk</sup>* mutants and wild-type *yw* flies were also used. In locomotor activity, flies with a single peak over the significance line in a Chi-squared analysis were scored as rhythmic, which was confirmed by visual inspection of the actograms<sup>33</sup>. Data shown were obtained from at least three independent experiments. Statistical analysis included was performed with a Student's *t*-test.

**Dissection and immunofluorescence.** Flies were entrained in a 12-h light–dark cycle at 25 °C and young (0–3-day old) adult flies were decapitated during the first day in constant darkness at circadian time (CT) 2 and CT 14. Brains were fixed in 4% paraformaldehyde in phosphate buffer and then rinsed three times in PBS-Triton (PT). Brains were then blocked in 7% goat serum in PT for 45 min at 25 °C. After the blocking step tissue was incubated with primary antibodies overnight at 4–8 °C. The primary antibodies used were rabbit anti-PER (1:800, donated by the M. Rosbash laboratory) and rat anti-PDF (1:800, generated in our laboratory). The secondary antibodies used were Cy2-conjugated donkey anti-rabbit and Cy3-conjugated anti-rat (Jacksons Immunoresearch) diluted to a final concentration of 1:250, incubated for 2 h at 25 °C. After staining, brains were washed four times for 15 min each and mounted in 80% glycerol (in PT). Images were taken on a Zeiss Pascal confocal microscope. Nuclear quantification of PER immunoreactivity was performed employing the Image J software.

**Circadian rhythm analysis in *Arabidopsis*.** For leaf movement analysis, plants were entrained in a light–dark cycle, transferred to continuous white fluorescent light and the position of the first pair of leaves was recorded every hour for 5–6 days<sup>34</sup>. Period estimates were calculated with Brass 3.0 software (Biological Rhythms Analysis Software System, available from <http://www.amillar.org>) and analysed with the FFT-NLLS suite of programs, as described previously<sup>35,36</sup>. An ANOVA followed by Tukey's Multiple Comparison Test were used for comparisons among genotypes. For bioluminescence assays, wild-type plants and *prmt5-5* mutants carrying the *CAB2::LUC<sup>36</sup>* or the *TOC1::LUC* reporter<sup>37</sup> were grown in a 12:12 h light–dark cycle of cool white fluorescent light and transferred to continuous white fluorescent light for 5–6 days. Seeds carrying the bioluminescence reporters were provided by S. L. Harmer. Bioluminescence rhythms were detected with a microplate luminometer LB-960 (Berthold Technologies) and analysed with Mikrowin 2000 (version 4.29) software (Mikrotek Laborsysteme). Luminescence from individual traces was analysed with Brass 3.0 software<sup>36</sup>. The phase distribution of clock-regulated genes was evaluated with Phaser (<http://phaser.cgrb.oregonstate.edu>)<sup>38</sup>.

**Flowering time analysis.** Flowering time was estimated by counting the number of rosette leaves at the time of there being a 1-cm-high flower bolt. The experiments were performed in a 16:8 h light–dark cycle at a constant temperature of 22 °C.

**qRT-PCR expression analysis.** RNA samples were subjected to a DNase treatment with RQ1 RNase-Free DNase (Promega). cDNA derived from this RNA was synthesized using Invitrogen SuperScript III and oligo-dT primer. The synthesized cDNAs were amplified with FastStart Universal SYBR Green Master (Roche) using the 7500 Real Time PCR System (Applied Biosystems) cyclor. *ACTIN 8* and *ribosomal protein 49 (rp49)* transcripts were used as normalization controls for *Arabidopsis* and *Drosophila*, respectively.

***Arabidopsis* gene expression microarray analysis.** Total RNA was extracted from aerial tissue of plants grown in constant white fluorescent light at 22 °C, without prior entrainment to light–dark or temperature cycles. Each sample consisted of 3–4 plants, to reduce biological variation. Five micrograms of RNA from 21-day-old plants of the wild-type and *prmt5-5* mutant genotypes was processed and hybridized to Affymetrix GeneChip *Arabidopsis* ATH1 Genome Arrays

according to the manufacturer's instructions. Microarray signals were made comparable by scaling the average overall signal intensity of all probe sets to a target signal of 250. Data were analysed using MASS5. We considered for further analysis only those genes having a present call in all samples of either wild-type or *prmt5-5* mutant plants. The statistical significance of signal differences was evaluated by SAM software<sup>39</sup>. We performed a two-class unpaired *t* test on the signal values, and 100 permutations were used to estimate the false discovery rate. Setting the delta cutoff value at 1.2, and establishing a minimum fold change of 2 between genotypes, 171 genes were found to be significantly regulated by PRMT5 with a false discovery rate of 3.08%.

**Whole genome tiling array analysis.** For *Arabidopsis* tiling arrays, plants were grown under continuous light for three weeks without prior light or temperature entrainment. For *Drosophila* tiling arrays, flies were grown and maintained at 25 °C in vials containing standard cornmeal medium, and kept in a 12:12 h light–dark cycle and transferred to constant darkness. Head collection and homogenization was done every three hours during the first day in constant darkness. RNA samples from different time points throughout a circadian cycle were pooled together and treated as one. GeneChip *Arabidopsis* Tiling 1.0R Array (Affymetrix) and GeneChip *Drosophila* Tiling 1.0R Array (Affymetrix) were processed according to standard Affymetrix protocols. For *Drosophila* array annotation, perfect match probes from the *Drosophila* tiling 1.0R array (Affymetrix) were megablasted against the *Drosophila* genome release version 5 with word size  $\geq 8$  and *E* value  $\leq 0.01$ . Single perfect matches, without a second partial match of  $>18/25$  bp, were selected, giving a total of 2,930,433 unique probes. These were mapped to annotated mRNAs as exon, intron, intergenic, or flanking probes that span an annotated boundary. Intergenic probes, flanking probes, and probes interrogating multiple transcripts were excluded from the *Drosophila* RNA data. The *Arabidopsis* tiling 1.0R array was annotated previously<sup>40</sup>. For both *Arabidopsis* and *Drosophila*, gene expression and splicing analysis was performed as previously described<sup>40</sup>. Log transformed intensity data from wild types and mutants were fitted with a linear model: intensity = genotype + error, where the genotype term contrasts wild types and mutants. Exonic splicing analysis used probe intensities corrected by mean gene expression. FDRs were determined by 20 permutations<sup>40</sup>.

**Bioinformatic analysis of donor splice-site sequences.** The genome-wide frequency of each nucleotide for each position of the 5'-splice-site sequence was obtained from SpliceRack<sup>41</sup>. The over- or underrepresentation of a particular nucleotide relative to its genome-wide frequency and *P* value was calculated using the hypergeometric test. Nucleotide frequencies were represented using the WebLogo software<sup>42</sup>.

**Radioactive PCR for *PRR9* and *per* splicing assessment.** Radioactive PCR amplification was performed containing 1.5 U of Taq polymerase (Invitrogen). Primers used for *per* amplification were taken from ref. 5. RT-PCR products were electrophoresed and detected by autoradiography. Radioactivity amounts per band were measured in a scintillation counter (Cerenkov method).

**High-resolution RT-PCR panels.** Plants were grown under continuous light for three weeks without prior light or temperature entrainment and RNA samples were obtained as described earlier. First-strand cDNA synthesis, PCR protocol and splicing analysis were previously described<sup>21</sup>.

**Western blot analysis.** Grind tissue in liquid nitrogen and resuspend the powder in 200–500  $\mu$ l of Lysis Buffer (50 mM Tris-HCl, pH 7.5, 150 mM NaCl, 1% Nonidet P-40, 0.5% deoxycholate and protease inhibitors; Roche) or RIPA buffer. Sample loading was made with 2 $\times$  Laemmli's buffer in 15–18% SDS-polyacrylamide gel electrophoresis gels. After transference to PVDF membranes the immunoblotting was made with Y12 and SYM10 antibodies according to manufacturer's recommendations.

**Sequential chromatin immunoprecipitation (Re-ChIP) assays.** Two-week-old seedlings were grown in a 12:12 h light–dark cycle and treated as previously described<sup>43</sup>. Before the elution from the beads, the immunoprecipitated complexes were released with 10 mM dithiothreitol and then diluted 20 times with Re-ChIP Buffer (20 mM Tris-HCl, pH 8.0, 150 mM NaCl, 2 mM EDTA, 1% Triton X-100, 1 mM phenylmethylsulphonyl fluoride, 1  $\mu$ g ml<sup>-1</sup> aprotinin, 1  $\mu$ g ml<sup>-1</sup> pepstatin A, 1  $\mu$ g ml<sup>-1</sup> antipain<sup>-1</sup>, 1  $\mu$ g ml<sup>-1</sup> leupeptin and 1  $\mu$ g ml<sup>-1</sup> chymostatin) and subjected again to the ChIP procedure (adapted from ref 44). The first immunoprecipitation was performed with anti-histone H4 and the second one (Re-ChIP) with anti-dimethyl-arginine symmetric (SYM10) antibodies (Upstate Biotechnology). DNA obtained was purified using a GFX PCR DNA and Gel Band Purification kit (GE Healthcare) following standard procedures. The amplified promoter region of the *FLC* gene (–523 to –273) was previously described to be subject to epigenetic control<sup>45</sup>. Two promoter regions of the *PRR9* gene were amplified: –621 to –443 and –61 to 83. PCR amplification products were electrophoresed in agarose gel and were stained with SYBR green (Sigma-Aldrich) following the manufacturer's recommendations. Gels were quantitative in the range of DNA concentrations used. Images were captured with the Kodak Digital Science

System, and quantification was performed with ImageQuant software (Molecular Dynamics) and Scion Image software. Here we show one representative of two independent experiments.

31. Alonso, J. M. *et al.* Genome-wide insertional mutagenesis of *Arabidopsis thaliana*. *Science* **301**, 653–657 (2003).
32. Murashige, T. & Skoog, F. A revised medium for rapid growth and bioassays with tobacco tissue cultures. *Physiol. Plant.* **15**, 473–497 (1962).
33. Rezával, C., Werbach, S. & Ceriani, M. F. Neuronal death in *Drosophila* triggered by GAL4 accumulation. *Eur. J. Neurosci.* **25**, 683–694 (2007).
34. Hicks, K. A. *et al.* Conditional circadian dysfunction of the *Arabidopsis* early-flowering 3 mutant. *Science* **274**, 790–792 (1996).
35. Plautz, J. D. *et al.* Quantitative analysis of *Drosophila period* gene transcription in living animals. *J. Biol. Rhythms* **12**, 204–217 (1997).
36. Millar, A. J., Carre, I. A., Strayer, C. A., Chua, N. H. & Kay, S. A. Circadian clock mutants in *Arabidopsis* identified by luciferase imaging. *Science* **267**, 1161–1163 (1995).
37. Strayer, C. *et al.* Cloning of the *Arabidopsis* clock gene *TOC1*, an autoregulatory response regulator homolog. *Science* **289**, 768–771 (2000).
38. Michael, T. P. *et al.* A morning-specific phytohormone gene expression program underlying rhythmic plant growth. *PLoS Biol.* **6**, e225 (2008).
39. Tusher, V. G., Tibshirani, R. & Chu, G. Significance analysis of microarrays applied to the ionizing radiation response. *Proc. Natl Acad. Sci. USA* **98**, 5116–5121 (2001).
40. Zhang, X., Byrnes, J., Gal, T., Li, W.-H. & Borevitz, J. Whole genome transcriptome polymorphisms in *Arabidopsis thaliana*. *Genome Biol.* **9**, R165 (2008).
41. Sheth, N. *et al.* Comprehensive splice-site analysis using comparative genomics. *Nucleic Acids Res.* **34**, 3955–3967 (2006).
42. Crooks, G. E., Hon, G., Chandonia, J.-M. & Brenner, S. E. WebLogo: a sequence logo generator. *Genome Res.* **14**, 1188–1190 (2004).
43. Perales, M. & Mas, P. A functional link between rhythmic changes in chromatin structure and the *Arabidopsis* biological clock. *Plant Cell* **19**, 2111–2123 (2007).
44. Métivier, R. *et al.* Estrogen receptor- $\alpha$  directs ordered, cyclical, and combinatorial recruitment of cofactors on a natural target promoter. *Cell* **115**, 751–763 (2003).
45. Bastow, R. *et al.* Vernalization requires epigenetic silencing of FLC by histone methylation. *Nature* **427**, 164–167 (2004).